

**Rapid #: -22884187**

CROSS REF ID: **20835208980003496**

LENDER: **UK3JU (University of Plymouth) :: Main Library**

BORROWER: **IEUOL (University of Limerick) :: Main Library**

TYPE: Article CC:CCG

JOURNAL TITLE: Ships and offshore structures

USER JOURNAL TITLE: Ships and Offshore Structures

ARTICLE TITLE: Friction stir welding induced residual stresses in thick steel plates from experimental and numerical analysis

ARTICLE AUTHOR: Hashemzadeh

VOLUME: 17

ISSUE: 5

MONTH:

YEAR: 2021

PAGES: 1053-1061

ISSN: 1744-5302

OCLC #:

Processed by RapidX: 7/25/2024 5:13:50 AM

---

This material may be protected by copyright law (Title 17 U.S. Code)

---



## Friction stir welding induced residual stresses in thick steel plates from experimental and numerical analysis

M. Hashemzadeh, Y. Garbatov, C. Guedes Soares & A. O'Connor

**To cite this article:** M. Hashemzadeh, Y. Garbatov, C. Guedes Soares & A. O'Connor (2022) Friction stir welding induced residual stresses in thick steel plates from experimental and numerical analysis, *Ships and Offshore Structures*, 17:5, 1053-1061, DOI: [10.1080/17445302.2021.1893531](https://doi.org/10.1080/17445302.2021.1893531)

**To link to this article:** <https://doi.org/10.1080/17445302.2021.1893531>



Published online: 04 Mar 2021.



[Submit your article to this journal](#)



Article views: 280



[View related articles](#)





[View Crossmark data](#)



Citing articles: 2 [View citing articles](#)



# Friction stir welding induced residual stresses in thick steel plates from experimental and numerical analysis

M. Hashemzadeh <sup>a</sup>, Y. Garbatov <sup>a</sup>, C. Guedes Soares <sup>a</sup> and A. O'Connor<sup>b</sup>

<sup>a</sup>Centre for Marine Technology and Ocean Engineering (CENTEC), Instituto Superior Técnico, Universidade de Lisboa, Lisboa, Portugal; <sup>b</sup>The Welding Institute, Granta Park, Cambridge, UK

## ABSTRACT

Friction stir welding induces a relatively low level of deflection, and residual stresses and recent advances in the welding technology has shown that friction stir welding may now be broadly used in steel welding leading to significant improvement of the welding quality for new constructions and repairs. In the present study experimental and numerical analyses of friction stir welding in thick steel plates are performed. A finite element model is developed, based on a new heat input source mathematical formulation, accounting for the welding transient thermo-mechanical process of the friction stir welding-induced residual stresses. The welding-induced residual stresses, estimated by the new developed finite element model, are compared with the experiment. The present study shows that the newly developed heat source finite element model demonstrates an acceptable agreement between the numerical and experimental results. A sensitivity analysis concerning the essential governing parameters predicting the friction stir welding – induced residual stresses is also addressed.

## ARTICLE HISTORY

Received 27 October 2019  
Accepted 10 February 2021

## KEYWORDS

Friction stir welding; heat source; finite element method; experiment

## 1. Introduction

Friction stir welding (FSW) develops solid-state and low-temperature welding, which has been shown to provide weight-efficient, fatigue and corrosion-resistant joints in aluminium. FSW has been firstly reported by Thomas et al. (1991), and it was initially developed for aluminium structures. The recent advances in the welding technology showed that the initially claimed benefits might be achieved as discussed in (Lienert et al. 2003; Fujii et al. 2006; Paik 2009).

FSW is an alternative to the conventional types of welding. It generates less heat and thus induces smaller heat-affected zones, which leads to less deflection and residual stresses induced during welding. Therefore, the impact of this type of welding in reducing strength is much less (Magoga and Flockhart 2014). The low heat-input of FSW reduces the probability of hot-crack initiation and distortions. Furthermore, dissimilar alloys and materials can be welded, applying FSW technique (Patel et al. 2019) in all positions and directions (Chen and Kovacevic 2003). In principle, better weld quality is achieved by FSW compared to other welding techniques. Also, FSW covers an extensive range of thicknesses employing a fully automatic welding process.

The need to impose large forces, rigid constraints, weld gaps, and the associated cost are considered disadvantages of FSW. Furthermore, FSW is sensitive to the welding tool, and several studies reported the influence of the welding tool shapes and the corresponding impact (Shi et al. 2015; Su et al. 2015).

FSW is a complex and relatively new welding process that still needs to be investigated in improving its joining capacities.

Several experimental and analytical solutions were reported in analysing FSW for example, He et al. (2014) comprehensively reviewed the use of numerical analysis tools for analysing FSW.

The heat energy of FSW is generated by the friction of the tool shoulder located on the top surface of the welded joint (Thomas et al. 1991). Several studies have been performed to estimate the heat generation during FSW employing analytical solutions (Neto and Neto 2013).

The process of FSW may be analysed by simulating the friction during the welding, accounting for the friction coefficient, rotational and axial forces, that are subjected to the contact area employing the finite element method, (FEM). Chiumenti et al. (2013) adopted a fully coupled, thermo-mechanical solution. They used a sliding mesh (rotating together with the pin) around the tool in the stirring zone and kept the rest of the mesh of the sheet fixed. Accurate results were achieved from both thermal and mechanical analyses. Haghpanahi et al. (2013) established a new transient analytical solution, based on the Green's function method, to obtain the three-dimensional temperature field during welding. The temperature distribution was estimated for different stages of the welding process, including penetration, preheating, and cooling using FEM thought commercial software.

The friction model is reported for both aluminium (Bussu and Irving 2003; Bastier et al. 2008; Schmidt and Hattel 2008) and steel (Darvazi and Iranmanesh 2014; Medhi et al. 2015) and good results were reported with both materials.

Another alternative to simulate FSW in FEM is the thermo-mechanical analysis based on the moving heat source

implemented in the present study. Li and Liu (2014) presented the results based on the moving heat source, and demonstrated that the temperature distribution and longitudinal stresses have a good agreement with the experimental results, but in terms of transverse stresses, they were inconsistent.

Salloomi et al. (2013) used a sequential coupling of the thermal histories into the mechanical model considering an elastic-perfectly plastic metal behaviour following the classical metal plasticity theory and estimating the welding-induced temperature and residual stresses. Using the WELDSIM finite element code, Zhu and Chao (2004), estimated the welding-induced temperature distribution and residual stresses of FSW in thin plates employing the inverse method to estimate the thermal boundary condition in the transient thermomechanical analysis.

Most of the investigations performed regarding FSW in steel has been limited to 6mm plate thickness. In the present study, the feasibility of applying FSW to a butt-welded thick steel plate is analysed by an experimental investigation. The experimental study is regenerated by using FEM. A new heat source model based on an analytical solution has been developed to analyse FSW of thick plates. The developed model may be directly employed in the transient thermo-mechanical analysis to estimate the welding-induced temperature and residual stresses. The new heat source model developed for the FSW is based on the previous studies in the welding simulations reported in (Chen et al. 2014; Hashemzadeh et al. 2014, 2017, 2018).

The newly developed approach could be used to design the FSW process to estimate the acceptable ranges of governing parameters of welding in controlling the plasticisation and welding-induced residual stresses. Therefore, the developed approach may reduce the computational time of the welding simulation.

## 2. Experimental setup

To investigate the use of FSW in butt-weld thick plates of AH36 grades of steel, two plates of  $150 \times 2000 \times 12$  mm, were welded along the 2 m edge using the friction stir welding process and the welding-induced residual stresses were assessed. The FSW tools used for this study were hybrid W-Re/pcBN tools produced by MegaStir Inc. The polycrystalline cubic boron nitride (pcBN) tool technology is necessary to provide the required thermal stability, hardness, and strength needed at the elevated temperatures experienced in the FSW of steel. The tools specified for this project were of MegaStir's Q70 grade material, thus signifying that the material contained 70% pcBN in a tungsten rhenium binder. The MegaStir tools have a scroll feature on a stepped shoulder and are designed to be operated with zero tool tilt degrees.

The task of making friction stir welds in thick steel plates was approached in two steps. First, the operational parameters controlling the plasticisation of the steel are defined, and in the second step, the operational parameters governing the welding process are identified.

To accomplish stage 1, steel plates instrumented with surface mounted K type thermocouples, and an instrumented friction stir welding tool was plunged into the steel. The heat

generated by the rotating tool was measured via the thermocouples, and the softening of the steel as it undergoes plastic deformation by force transducers incorporated in the FSW machine. By measuring the temperatures and forces, the primary control parameters (tool rotation rate and tool plunge speed) were identified during the plastic deformation of the steel. Once the control parameters reach their operational values, the tool is plunged into the steel without breaking, and the adequacy of the softening of the steel allows it to flow around the tool, further grow-up the control parameters allow the tool to traversed along the joint line, maintaining adequate plastic deformation of the steel in the weld zone and consolidating the steel behind the tool forming a sound weld.

The plate surfaces were clamped to the FSW machine bed using standard machining type finger clamps. The welds were made in force control conditions. The force with which the tool was plunged into the steel plate was programmed into the machine and held constant. A vertical ( $F_y$ ) force of 90 kN was employed to make the welds. The welds were made at a tool traverse rate of 100 mm/min and a nominal tool rotation speed of 150 rpm. Small adjustments were made to the tool rotation speed during the welding when required to control the process stability. Argon at a flow rate of 14 l/min was used as a shielding gas to protect the FSW tool from oxidation during the welding process. The tool plunging to the specimen and extracting from the steel are illustrated in Figure 1.

Investigating the possibility of implementing FSW in thick steel plates is the main objective of the present study; therefore, full penetration of the weld is very important as a single pass is applied. Figure 2 shows a metallographic section through the weld in an AH36 plate. This section was used to examine the internal weld structure and verifying full penetration. It seems that a defect is observed during the test. These kinds of defects in FSW mainly occur because of the processing parameters, material, and tool shape (Buffa et al. 2009; Mohammedi et al. 2015; Abushanab and Moustafa 2018) and it could be solved by a metallurgical analysis which is not the concern of this work.

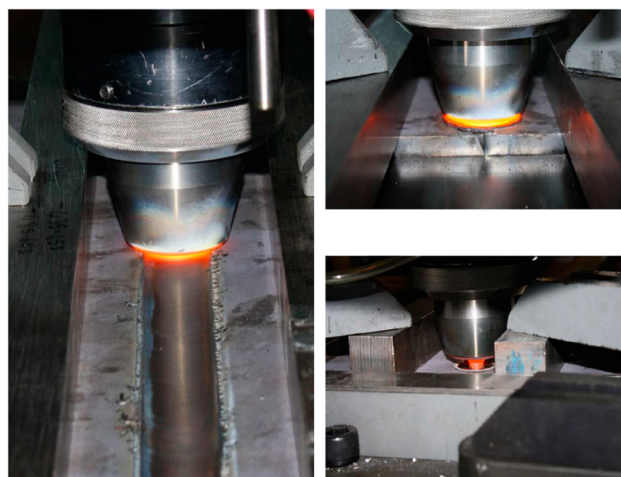


**Figure 1.** Tool and weld surface (left) and tool plunging to the specimen and extracting from the steel (right). (This figure is available in colour online.)



Figure 2. Metallographic section through the weld.

The welding-induced residual stresses were measured by using the centre hole drilling method. Fifty-micron aluminium oxide powder was used with an abrasive machine. The material was abraded using an air pressure of 4.8 bars. Five strain gauge rosettes of type FRS-2-11 were attached, as shown in Figure 3. Gauges were orientated so that the z-axis was parallel to the weld direction and the x-axis was transverse to the weld direction. The third element was at 135 degrees to both the z and x directions. The gauges were applied to bare polished steel using a thin layer of cyanoacrylate adhesive as the bonding agent and were wired to a computer-controlled measurement system using a three-wire quarter bridge configuration.

Following the procedure, (TWI 2009) the measured residual stresses were modified to account for plasticity effects as follows:

$$\sigma_{\text{residual}} = \frac{\sigma_{\text{measured}}}{0.28 \left( \frac{\sigma_{\text{measured}}}{0.65 \sigma_{\text{yield}}} \right) + 0.82} \quad (1)$$

where  $\sigma_{\text{measured}}$  is the residual stress measured using the centre hole drilling technique and  $\sigma_{\text{yield}}$  is the yield strength of the material.

### 3. Heat generated by FSW

In the present study, a code based on ANSYS Programme Development Language, APDL is developed to model the

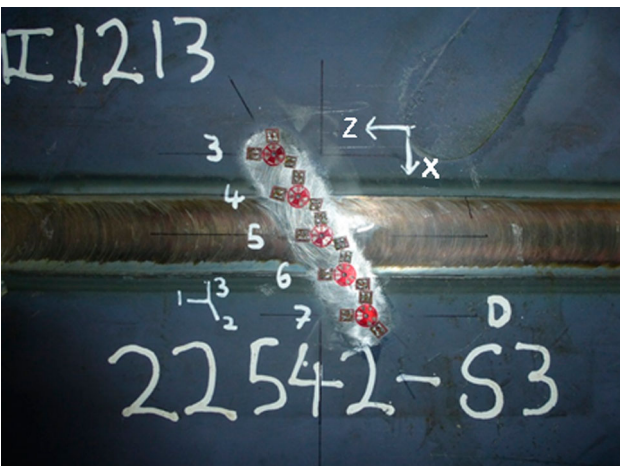


Figure 3. Strain gauge orientation. (This figure is available in colour online.)

FSW process by employing a transient thermo-mechanical analysis, where the temperature distribution during the welding process the welding-induced residual stresses and distortions are estimated.

In the thermo-mechanical analysis process, an appropriate mathematical model of the heat source as an input needs to be defined, which has crucial importance in the mechanical results. Based on the analytical solutions, it is tried to calculate the heat generation during FSW, and through a FE analysis a new heat input distribution in thick plate considering calculated generated heat in this section is developed (Section 6).

The heat is generated by the rotation and friction between the shoulder of the welding tool and the surface of the welded plates (see Figure 4). The heat is generated by friction, making plastic material in the welding area. Three principal mechanisms contribute to the heat source: friction at the shoulder-piece interface, friction at the probe-piece interface and plastic strain at the piece (Chen and Kovacevic 2003). The friction stir welding process mechanism is complex, and because of that, an accurate mathematical model of the heat source for FSW is challenging to be defined.

To estimate the heat generation during FSW, an analytical model is adopted in this paper to represent the heat source (Li and Liu 2014). The friction force  $f_k$ , is defined as the normal force  $N$ , is multiplied by the friction coefficient  $\mu$ :

$$f_k = \mu N \quad (2)$$

Furthermore, the work  $W$ , developed by friction, is defined as:

$$W = \mu N x \quad (3)$$

which generates heat defined as  $dW/dt$ :

$$Q = \frac{dW}{dt} = \mu N \frac{dx}{dt} \quad (4)$$

leading to:

$$Q = \int q dA = \int \frac{F}{A} \mu r^2 \omega dr d\theta \quad (5)$$

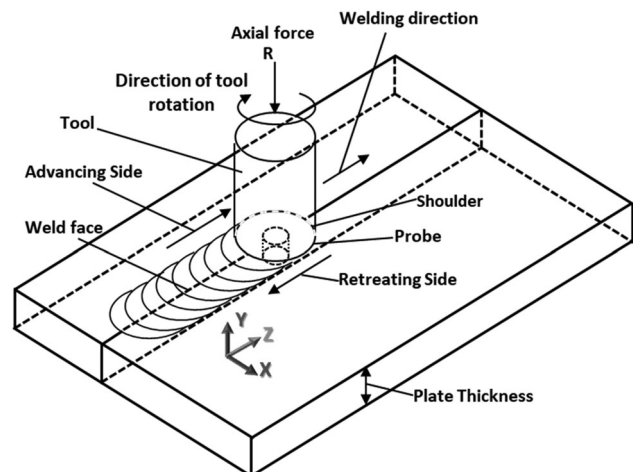


Figure 4. FSW process.



where

$$Q = \frac{2\pi \mu F \omega}{3 A} (r_2^3 - r_1^3) \quad (6)$$

Considering that  $W_{rpm} = (2\pi/60)W_{rad/s}$  and  $A = \pi r_2^2$ , then the heat can be expressed as:

$$Q = \frac{4\pi}{180} \mu F \omega \frac{(r_2^3 - r_1^3)}{r_2^2} \quad (7)$$

Figure 5 shows the definition of the parameters included in Equation (7).

The heat intensity is defined as:

$$q_{\max} = \frac{Q}{A} = \frac{1}{45} \mu F \omega \frac{(r_2^3 - r_1^3)}{r_2^2(r_2^2 - r_1^2)} \quad (8)$$

where  $F$  is the downward force,  $\omega$  is the rotational tool speed,  $r_1$  is the actual probe radius, and  $r_2$  is the assumed slip surface radius. The tool translational motion contribution has a negligible impact (Russell and Sheercliff 1999), but in the study is also considered and calculated as:

$$dq_p = \mu \sigma dA_c \bar{r}_p \omega \rightarrow Q_p = 2\pi \bar{r}_p^2 h_p \mu \sigma \omega \quad (9)$$

where  $\sigma = F/S_c \times r_1^2/r_2^2$  and  $S_c = \pi r_p h_p$ .

#### 4. Finite element modelling

In the present study, the friction stir welding process in thick plates is analysed using the FEM employing the transient thermo-mechanical analysis. Welding of thick plates is very challenging and may create cracks and significant distortions. FSW is capable of joining structural components with significantly less distortion than conventional fusion welding. Based on FEM, a semi-analytical solution of heat source is developed

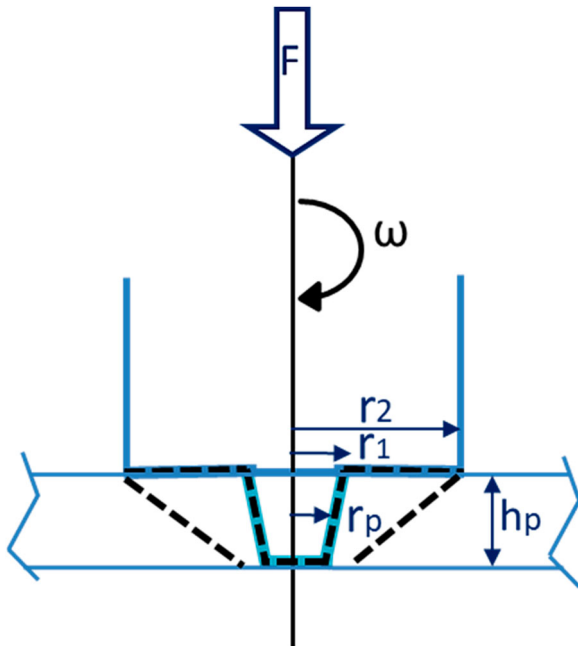


Figure 5. Weld nugget parameters. (This figure is available in colour online.)

for simulating FSW to estimate the heat generation and residual stresses in butt-welded thick plates.

The heat transfer in FSW is a complex process, and by increasing the plate thickness, a situation is more complicated as three-dimensional effects are involved in the problem. In the present study, considering a simplified analytical solution, which is explained in Section 4, three case studies considering three different models of a heat source (as shown in Section 6) are implemented to investigate thermal-mechanical behaviour of FSW in thick plates. To determine an appropriate heat source model estimated that welding induced residual stresses calculated by thermo-mechanical analysis are compared with real measurements from the experimental study, and a comprehensive discussion is presented.

To develop the finite element model, the indirect thermo-mechanical analysis is implemented in the present study. In this regard, first, a heat source model is defined to simulate the moving thermal load (see Section 6). Then by running a thermal analysis, the temperature distribution of each nodal location is estimated. In the next step, which is a mechanical analysis, the thermal model containing the equivalent finite thermal elements are replaced by mechanical elements and the temperatures obtained from the thermal analysis are applied as body loads. In other words, the geometry, nodal locations and the coordinate system of these elements are coinciding with the corresponding thermal elements. Subsequently, mechanical boundary conditions are applied. Then by running mechanical analysis, welding-induced residual stresses and distortions are calculated.

Finite element software (Ansys 2013) is employed to perform the transient thermo-mechanical analysis. The finite element model is generated by eight-node three-dimensional brick thermal elements, Solid 70. The element has eight nodes with a single degree of freedom, temperature, at each node. The element can also compensate for a mass transport heat flow from a constant velocity field. For the mechanical analysis, a structural element defined by eight nodes, i.e. SOLID185 is used for the three-dimensional modelling of the welded plates. Each node of the element has three degrees of freedom: nodal translations in the  $x$ ,  $y$ , and  $z$  directions. The element supports an analysis of plasticity, large deflection, considerable strain, stress stiffening, creep and swelling.

The geometry of the FE model and the structural boundary conditions are shown in Figure 6. The mechanical analysis

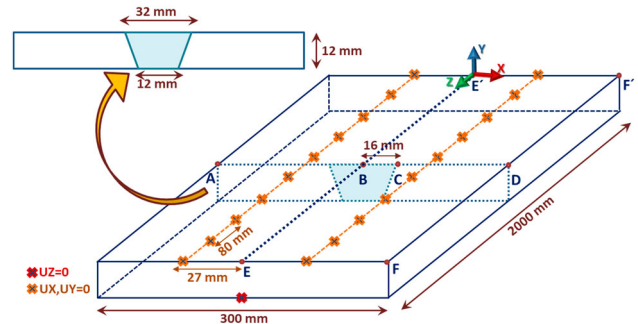


Figure 6. Finite element model and structural boundary conditions. (This figure is available in colour online.)

**Table 1.** Temperature-dependent material properties, ASTM A36 carbon steel (Chang and Teng 2004).

$T$ °C	$C$ J/Kg°C	$K$ W/m°C	$A$ $\mu\text{m/m}^\circ\text{C}$	$\sigma_y$ MPa	$E$ GPa
20	450	51	11.2	380	210
100	475	50	11.8	340	195
210	530	49	12.4	320	195
330	560	46	13.1	262	185
420	630	41	13.6	190	168
540	720	38	14.1	145	118
660	830	34	14.6	75	52
780	910	28	14.6	40	12
985	1055	25	14.6	38	11.8
1320	2000	32	14.6	28	10.4
1420	2100	42	14.6	25	10.2
1500	2150	42	14.6	20	10

boundary conditions are modelled as constraints avoiding transverse and vertical displacements of the surface. Nodes located with a distance of 27 mm from the weld path and at each 80 mm distance in the longitudinal direction are constrained. Constraints in the FE model represent the real experimental conditions. The welding line's endpoint is fixed in the longitudinal direction, preventing displacement in the  $z$ -direction.

A fine mesh is applied in the welding area to achieve a more accurate heat flux distribution. The finite element is composed of around 24,000 solid elements. The environmental temperature for the analysis, given as a thermal boundary condition is considered equal to 20°C. The initial temperature of the welded plates is assumed to equal to the ambient temperature. Six layers have been generated through the thickness of the welded plates. A common type of marine steel, ASTM A36 grade is used in the present study. To model the material characteristics, temperature-dependent material properties are implemented to consider the phase changing during the welding process. The temperature-dependent material properties of the ASTM A36 steel used in the analysis are presented in Table 1.

It is assumed that the heat energy is constant during welding, but the centre of the heat source is moved as a function of time. The surfaces of the butt-welded plates are subjected to heat convection, while the part of the plate, which is in contact with the heat source, is subjected to a heat flux instead.

## 5. Transient thermo-mechanical analysis

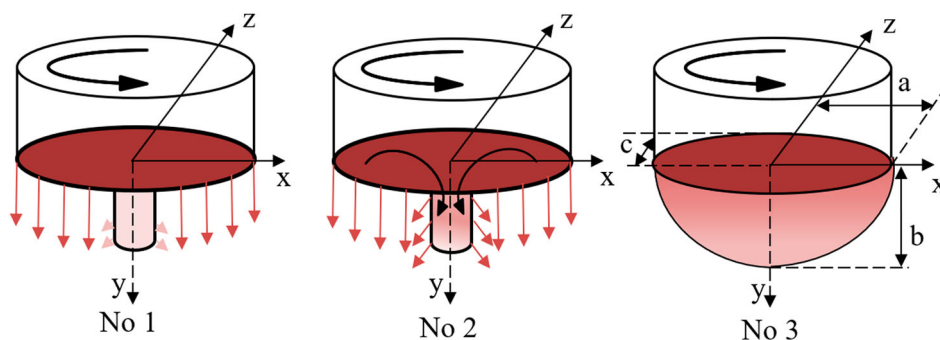
The present study aims to determine an appropriate heat source model for FSW that can be implemented directly in

the transient thermo-mechanical analysis. In this regard, three different heat input models of FSW presented in three different case studies (as shown in Figure 7) are developed and analysed in this section. To determine the accuracy of results from applying each heat model in thermo-mechanical analysis, calculated welding induced residual stresses are compared to measured residual stresses for both longitudinal and transverse residual stress.

The investigation started with the first model (No1 in Figure 7) based on the analytical solution. The heat generation, which is calculated for pin and shoulder in Section 4, is directly modelled in the FEM. By applying Equation (8) and (9) as heat source model in programming by the APDL code, the transient thermo-mechanical analysis was performed, and the induced welding temperature and residual stresses are calculated. The calculated heat generation of the pin in Section 4 showed a low amount of the heat energy; therefore, in model No1, the main part of heat generation belongs to the friction work of the shoulder. Figure 8 shows that the numerically estimated transverse component of the residual stresses (across to the weld toe) is quite identical with the experimentally measured. However, the longitudinal component of the residual stresses (parallel to the weld toe) has a more significant scatter. However, the maximum value of the tensile and compressive residual stress is close to the experiment.

From the result of the first model, it could be concluded that as in the first model the heat generated by the pin is negligible, the material located in the area near to the bottom of the plate does not reach to the plastic zone in the FE analysis. It means that the welding does not occur theoretically in this zone, which is the proof of the weakness of model No1 in FE modelling of FSW in thick plate. Therefore, for designing the new case study, it is assumed that the equal heat generated by shoulder could be considered for the pin due to the conduction flow in the tool (model No 2, Figure 7). It is considered that the amount of heat is reduced as a function of the distance from the plate surface, by running the thermo-mechanical analysis for the second heat source model, more accurate results achieved from FEM. Figure 9 shows for both longitudinal and transverse residual stresses the numerical results are coinciding with the experiment; however, there is an incompatibility in transverse residual stress distribution.

The third model is developed based on the achievement of the second case study, and the new ellipsoidal model, which could describe the FSW heat generation. Analysing the result

**Figure 7.** Three heat source models. (This figure is available in colour online.)

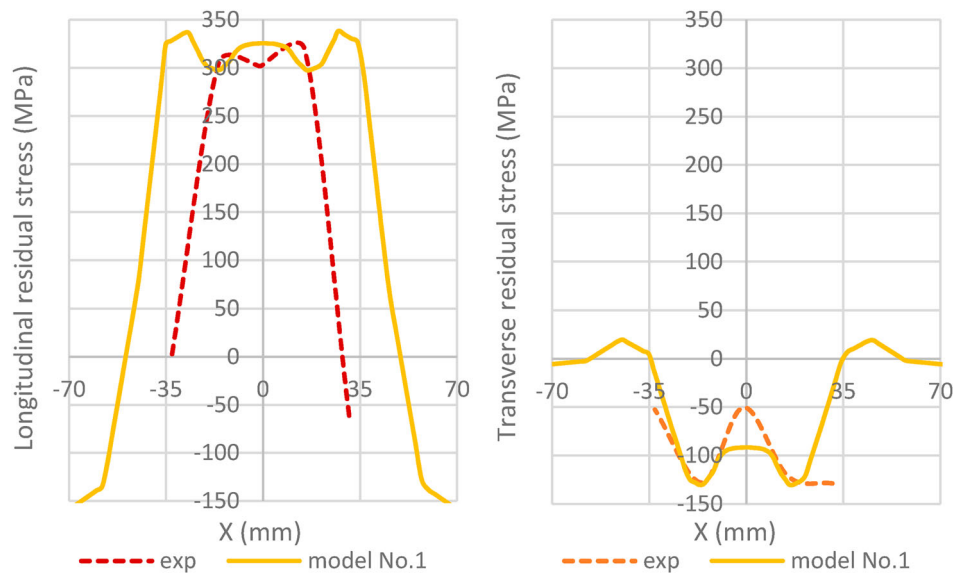


Figure 8. Residual stresses, model no 1. (This figure is available in colour online.)

based on model No 2 (see Figure 7), it is concluded that the heat flow in the thick plate has volumetric dependence. Therefore, a third model is developed as an ellipsoid shape to model the three-dimensionality of the heat input source:

$$q(x, y, z) = q_{\max} \exp\left(-\frac{2x^2}{r_2^2} - \frac{2y^2}{h_p^2} - \frac{2z^2}{r_2^2}\right) \quad (10)$$

where  $x$ ,  $y$  and  $z$  are the local coordinates of the ellipsoid model aligned with the weld.  $q_{\max}$  is calculated by Equation (7),  $r_2$  and  $h_p$  are the shoulder radius and pin height respectively. By implementing the new ellipsoid equation in thermo-mechanical analysis, the acceptable result for both longitudinal and transverse residual stress is achieved comparing with experiment (Figure 10). Furthermore, the transverse residual stress distribution result from employing model No 3 has a more accurate pattern than the experiment.

A sensitivity analysis concerning both boundary conditions and finite element size was performed concluding that the BCs are essential as the welding material is plastic and very sensitive to the loading and fixed nodal points should be applied along the length of the plate on a distance of  $2r_2$  or  $3r_2$ . The dimension of the finite element along the weld should be about  $r_2/2$  or  $r_2$ , considering that the maximum temperature during the welding process does not exceed the melting point of the material.

Figures 8–10 illustrate the residual stress distribution for longitudinal and transverse residual stresses measured experimentally and calculated numerically to compare the accuracy of the implementation of three different heat source models. Some discrepancies have been observed between the results obtained from the FE model and the experimental measurements. The differences occur due to several reasons. However, the main reason is probably related to the use of equal

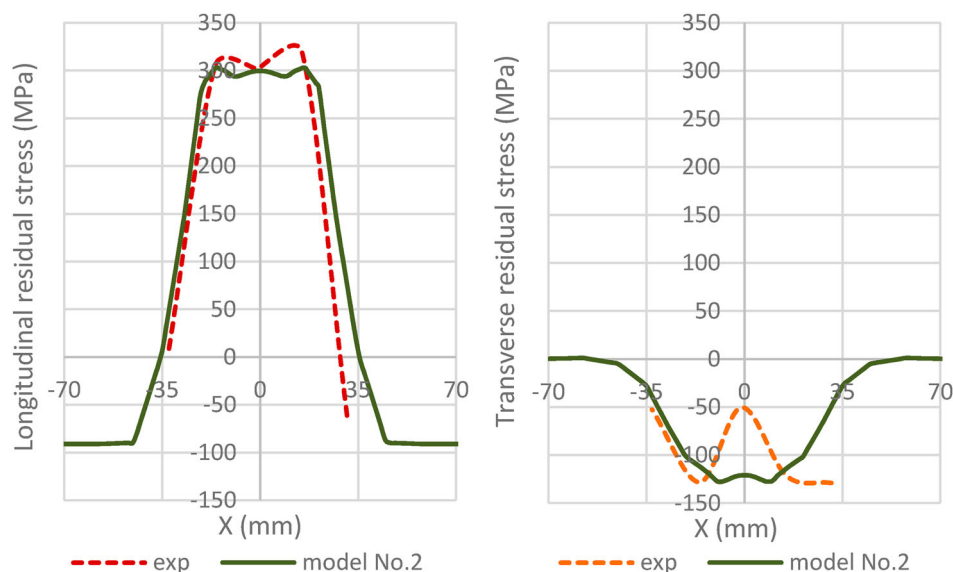


Figure 9. Residual stresses, model no 2. (This figure is available in colour online.)



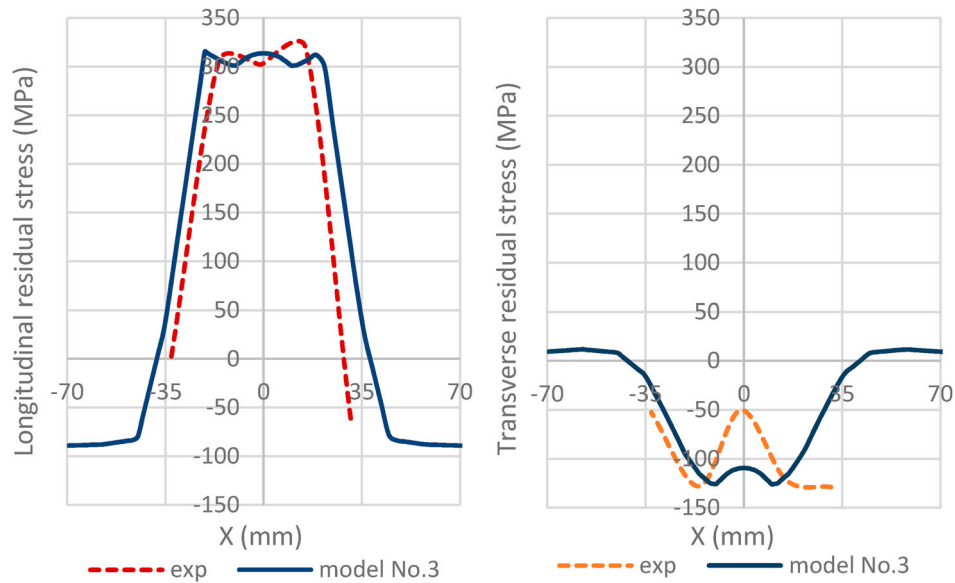


Figure 10. Residual stresses, model no 3. (This figure is available in colour online.)

Table 2. FEM and experimental results.

	Longitudinal tensile residual stress		Transverse compressive residual stress
	Stresses	Tensile width	
Experiment	318.8 MPa	61.43 mm	-119.36 MPa
Case study no 1	338.39 MPa	99.12 mm	-130.35 MPa
error	6.145%	61.37%	9.21%
Case study no 2	294.71 MPa	71.15 mm	-127.65 MPa
error	7.56%	15.83%	6.95%
Case study no 3	302 MPa	72.09 mm	-125.82 MPa
Error	5.27%	17.36%	5.41%

modelling factors and the same element sizes in the finite element models for the three heat source models. Furthermore, real physical factors and the simplification applied in the FE modelling may cause a difference between the numerical and experimental results.

The mechanical analysis results from the FE analysis for the three case studies and the experimental results are summarised and presented in Table 2. Considering the effect of pin contribution, it can be observed has significant improvement impact on thermo-mechanical analysis results. Applying the new

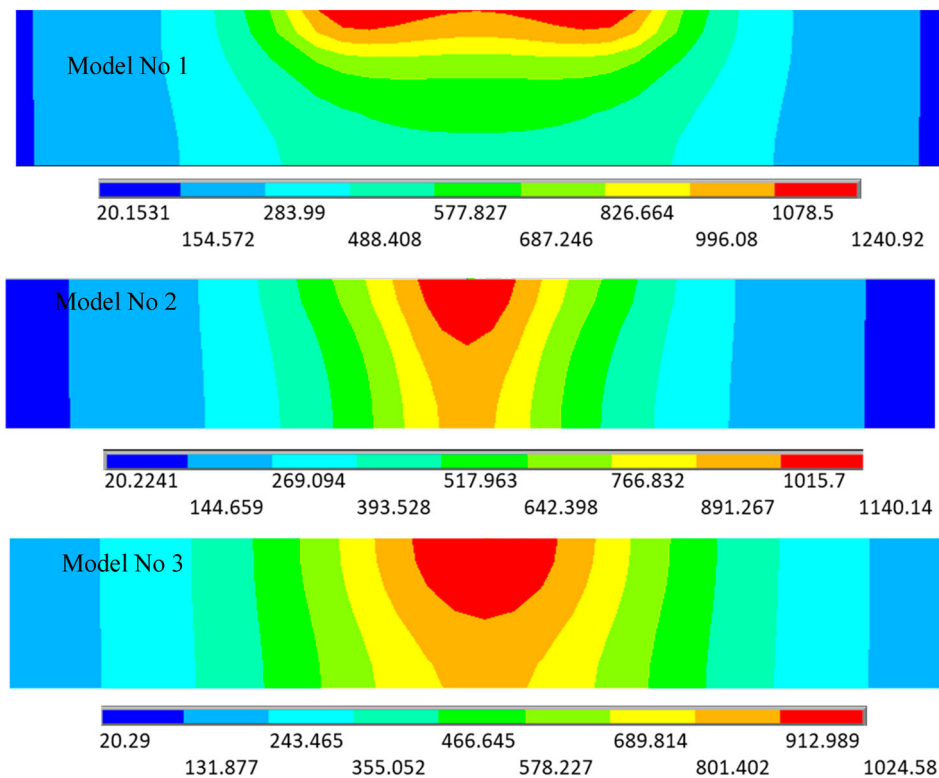


Figure 11. Temperature distribution in the cross-section. (This figure is available in colour online.)

ellipsoid heat source model in transient thermo-mechanical analysis promotes reliable estimates of residual stresses for both longitudinal and transverse stress components.

Figure 11 shows the temperature distribution in the welded plates' cross-section for the three cases studied here. The heat input model No1 causes lower temperature through the thickness. It means that by considering the heat only on the surface, contacted by the shoulder of the tool, a plastic phase is not reached in the material located in the bottom of the thick plates. However, Figure 11 shows that the thermal analysis performed for model No2 and No3 has more reliable results. It seems that the temperature distribution from these models has a smooth gradient through the thickness. It is noted that the maximum temperature achieved from the FEM analysis is controlled by the maximum temperature (around 1200°C), which is recorded by thermocouples during the experiment.

## 6. Conclusion

The present work investigates the residual stress induced by FSW of butt-welded thick plates using the experimental and numerical approaches.

The experimental study was carried out to investigate the possibility of implementing FSW in thick steel plates and collecting data to verify the numerical analysis. The experimental study observed that the friction stir welding was produced by employing a large vertical force (90kN), but the smooth weld face and deep weld penetration were achieved, which presented good weld quality in thick plates by implementing FSW.

In the present study to calculate the FSW residual stress, the transient thermo-mechanical method was used. In this regard, to develop a thermal analysis of the moving heat that could describe FSW, three models were developed and implemented in thermo-mechanical analysis, and the result accuracy of each model was measured compared to the experiment.

It was concluded from FE analysis that the newly developed ellipsoid model is an appropriate heat source model for analysing the FSW of butt-welded thick plates.

As an advantage of the present work, the newly developed approach may be used to design the FSW process to estimate the acceptable ranges of governing parameters of welding in controlling the plastification and welding-induced residual stresses.

The sensitivity analysis concluded that the boundary conditions have a significant impact on the welding-induced residual stresses.

## Acknowledgements

This work has been conducted within the project MOSAIC – Materials Onboard: Steel Advancements and Integrated Composites, which was partly supported by the European Commission under the FP7-SST-2012-RTD-1 contract. This work contributes to the Strategic Research Plan of the Centre for Marine Technology and Ocean Engineering (CEN-TEC), which is financed by the Portuguese Foundation for Science and Technology (Fundação para a Ciência e a Tecnologia - FCT) under contract UIDB/UIDP/00134/2020.

## Disclosure statement

No potential conflict of interest was reported by the author(s).

## Funding

This work was supported by Fundação para a Ciência e a Tecnologia - FCT [grant number SFRH/BD/97682/2013].

## ORCID

M. Hashemzadeh  <http://orcid.org/0000-0002-2207-1104>

Y. Garbatov  <http://orcid.org/0000-0001-7308-2586>

C. Guedes Soares  <http://orcid.org/0000-0002-8570-4263>

## References

- Abushanab WS, Moustafa EB. 2018. Detection of friction stir welding defects of Aa1060 aluminum alloy using specific damping capacity. *Materials*. 11(12):2437.
- Ansys. 2013. Online manuals. Release 2013.
- Bastier A, Maitournam MH, Roger F, Dang Van K. 2008. Modelling of the residual state of friction stir welded plates. *J Mater Process Technol*. 200(1-3):25–37.
- Buffa G, Campanile G, Fratini L, Prisco A. 2009. Friction stir welding of lap joints: influence of process parameters on the metallurgical and mechanical properties. *Mater Sci Eng A*. 519(1-2):19–26.
- Bussu G, Irving PE. 2003. The role of residual stress and heat affected zone properties on fatigue crack propagation in friction stir welded 2024-T351 aluminium joints. *Int J Fatigue*. 25(1):77–88.
- Chang PH, Teng TL. 2004. Numerical and experimental investigations on the residual stresses of the butt-welded joints. *Comput Mater Sci*. 29:511–522.
- Chen BQ, Hashemzadeh M, Garbatov Y, Guedes Soares C. 2014. Numerical and parametric modeling and analysis of weld-induced residual stresses. *Int J Mech Mater Des*. 11(4):439–453.
- Chen CM, Kovacevic R. 2003. Finite element modeling of friction stir welding – thermal and thermomechanical analysis. *Int J Mach Tools Manuf*. 43(13):1319–1326.
- Chiumenti M, Cervera M, Agelet De Saracibar C, Dialami N. 2013. Numerical modeling of friction stir welding processes. *Comput Methods Appl Mech Eng*. 254:353–369.
- Darvazi AR, Iranmanesh M. 2014. Thermal modeling of friction stir welding of stainless steel 304 L. *Int J Adv Manuf Technol*. 75(9-12):1299–1307.
- Fujii H, Cui L, Tsuji N, Maeda M, Nakata K, Nogi K. 2006. Friction stir welding of carbon steels. *Mater Sci Eng A*. 429(1-2):50–57.
- Haghpasahi M, Salimi S, Bahemmat P, Sima S. 2013. 3-D transient analytical solution based on green's function to temperature field in friction stir welding. *Appl Math Model*. 37(24):9865–9884.
- Hashemzadeh M, Chen BQ, Guedes Soares C. 2014. Comparison between Different heat source types in thin-plate welding simulation. In: Guedes Soares C, López Peña F, editors. *Developments in maritime transportation and exploitation of sea resources*. London: Taylor & Francis; p. 329–336.
- Hashemzadeh M, Chen BQ, Guedes Soares C. 2018. Evaluation of multi-pass welding-induced residual stress using numerical and experimental approaches. *Ships Offsh Struct*. 13(8):847–856.
- Hashemzadeh M, Garbatov Y, Guedes Soares C. 2017. Analytically based equations for distortion and residual stress estimations of thin butt-welded plates. *Eng Struct*. 137:115–124.
- He X, Gu F, Ball A. 2014. A review of numerical analysis of friction stir welding. *Prog Mater Sci*. 65:1–66.
- Li H, Liu D. 2014. Simplified thermo-mechanical modeling of friction stir welding with a sequential Fe method. *Int J Model Optim*. 4(5):410.
- Lienert T, Stellwag Jr W, Grimmert B, Warke R. 2003. Friction stir welding studies on mild steel. *Weld J New York*. 82(1):1S.

- Magoga T, Flockhart C. **2014**. Effect of weld-induced imperfections on the ultimate strength of an aluminium patrol boat determined by the Isfem rapid assessment method. *Ships Offsh Struct.* 9(2):218–235.
- Medhi T, Saha Roy B, Debbarma S, Saha SC. **2015**. Thermal modelling and effect of process parameters in friction stir welding. *Mater Today Proc.* 2(4-5):3178–3187.
- Mohammadi J, Behnamian Y, Mostafaei A, Gerlich AP. **2015**. Tool geometry, rotation and travel speed effects on the properties of dissimilar magnesium/aluminum friction stir welded lap joints. *Mater Des.* 75:95–112.
- Neto DM, Neto P. **2013**. Numerical modeling of friction stir welding process: a literature review. *Int J Adv Manuf Technol.* 65(1):115–126.
- Paik JK. **2009**. Buckling collapse testing of friction stir welded aluminum stiffened plate structures. Ship Structure Committee Report, SSC-456. Washington DC.
- Patel NP, Parlikar P, Singh Dhari R, Mehta K, Pandya M. **2019**. Numerical modelling on cooling assisted friction stir welding of dissimilar Al-Cu joint. *J Manuf Process.* 47:98–109.
- Russell MJ, Sheercliff HR. **1999**. Analytic modeling of microstructure development in friction stir welding. Proceedings of the first international symposium on friction stir welding, 1999 Thousand Oaks, CA, USA.
- Salloomi KN, Sabri LA, Hamad YM, Mohammed SN. **2013**. 3-Dimensional nonlinear finite element analysis of both thermal and mechanical response of friction stir welded 2024-T3 aluminum plates. *J Inf Eng Appl.* 3(9):6–15.
- Schmidt HB, Hattel JH. **2008**. Thermal modelling of friction stir welding. *Scr Mater.* 58(5):332–337.
- Shi L, Wu CS, Liu HJ. **2015**. The effect of the welding parameters and tool size on the thermal process and tool torque in reverse dual-rotation friction stir welding. *Int J Mach Tools Manuf.* 91:1–11.
- Su H, Wu CS, Bachmann M, Rethmeier M. **2015**. Numerical modeling for the effect of pin profiles on thermal and material flow characteristics in friction stir welding. *Mater Des.* 77:114–125.
- Thomas W, Nicholas E, Needham J, Murch M, Temple-Smith P, Dawes C. **1991**. Friction stir butt welding. International Patent Application No. Pct/Gb92. GB Patent application No. 9125978.8.
- TWI. **2009**. Procedure for residual stress measurement using the centre hole rosette gauge method: TWI procedure no. Si-Str-P3. Rev. 3.2, The Welding Institute. February 2009: The Welding Institute. Rev. 3.2, February 2009.
- Zhu X, Chao Y. **2004**. Numerical simulation of transient temperature and residual stresses in friction stir welding of 304 l stainless steel. *J Mater Process Technol.* 146(2):263–272.